Charging of multiple grains in subsonic and supersonic plasma flows

IOP Publishing
Plasma Physics and Controlled Fusion
Plasma Phys. Control. Fusion **57** (2015) 014019 (8pp)
doi:10.1088/0741-3335/57/1/014019

Charging of multiple grains in subsonic and supersonic plasma flows

D Block[1] **and W J Miloch**[2]

[1] IEAP, Christian-Albrechts-Universität, D-24098 Kiel, Germany
[2] Department of Physics, University of Oslo, Box 1048 Blindern, N-0316 Oslo, Norway

E-mail: w.j.miloch@fys.uio.no

Received 27 June 2014, revised 9 September 2014
Accepted for publication 19 September 2014
Published 28 November 2014

Abstract
The role of wake effects in the charging of dust grains by plasmas with subsonic and supersonic ion flows is studied with numerical simulations. Significant ion focusing which is common for supersonic flows is also observed for subsonic regimes. In both regimes, the charge on a downstream grain aligned with the flow depends linearly on the intergrain distance. For subsonic flows and systems with several grains, the complex ion dynamics can lead to significant modifications of the charge on grains located close to the boundary of a dust lattice and the charge distribution on the grains depends on the detailed grain arrangement. The studies are carried out with DiP3D, a self-consistent particle-in-cell code (Miloch 2010 *Plasma Phys. Control. Fusion* **52** 124004; Miloch and Block 2012 *Phys. Plasmas* **19** 123703).

Keywords: plasma, dust, wake, charge

(Some figures may appear in colour only in the online journal)

1. Introduction

Complex plasmas i.e. plasmas containing finite-sized dust grains, have attracted much attention in the last two decades [1]. Most studies investigated the strong coupling regime and used the possibility to access the individual grain dynamics experimentally [2, 3]. This approach has offered fascinating views on various dynamical processes at a kinetic rather than the well-known statistical level [1, 4, 5]. For this purpose complex plasmas are most often described by a one-component approach [6, 7]. The underlying idea is that the ambient plasma is assumed to provide enough electrons and ions to charge all dust grains identically. Combined with the fact that all dust dynamics are several orders of magnitude slower than the ion and electron dynamics, the only remaining plasma property in a one-component description of a complex plasma is the Debye shielding of the dust grains.

Nevertheless, dust charging and shielding are fundamental problems in complex plasmas. At usual laboratory conditions, dust grains are levitating above an electrode or are found in other regions with notable electric fields. Thus they are usually exposed to a directed flow of ions. From the sheath region in rf-discharges it is well known that the flowing plasma gives rise to wakes behind dust grains and that the resulting wakefield strongly affects the dynamics of other charged dust grains [3, 5, 8–12]. A good understanding of the interaction of a single grain with flowing plasma is already important to aim towards an appropriate description of the collective interactions in complex plasmas. Thus, much effort has been directed towards analytical [13–18] and numerical [19–24] studies of dust grain charging in plasma flows.

In most laboratory conditions, dust grains experience sonic or supersonic ion flows. At such conditions, the dust charge and potential agree in general with the shifted orbit-motion-limited theory and capacitance models [25–27]. The wakefield of a single grain can be successfully studied with the linear response theory as well as with numerical simulations using particle-in-cell codes [17, 19, 22, 23, 27–29]. With such simulations, in which the plasma particle trajectories are followed in self-consistent fields, it has been confirmed that a negatively charged grain causes an electrostatic lensing of ions into the wake region. This process is often termed *ion focusing* [3, 20, 30]. Good agreement between analytical solutions and numerical simulations of the wake field [16, 31] proves that its size and shape are well understood.

Unfortunately, this changes as soon as pairs or groups of dust grains are investigated. In supersonic flows, dust grains tend to form chains in the direction of the flow. The plasma response in such a wake allows for non-reciprocal forces between dust grains where the motion of the downstream grain is controlled by the upstream one but not vice versa [8, 10, 32]. While the preference for dust chains has been explained with the positive space charge downstream of a grain very early [33], the decharging of the downstream grain in the wake and the role of this process on the grain dynamics and their alignment with the flow have only recently been investigated [31, 34]. Fortunately, different simulation approaches and experiments on dust pairs now confirm that the downstream grain is significantly decharged by the enhanced ion flow which is produced by the electrostatic lensing by the upstream grain. Thus these results nicely extend the single grain picture. However, they raise a question about how larger groups of dust grains will charge and whether their charges can be predicted.

In many experimental situations dust grains are exposed to subsonic ion flows. These include dust grains that are located far in the pre-sheath from electrodes, naturally occurring complex plasmas and experiments under microgravity conditions [1, 2]. Although such conditions are ubiquitous, to date very few studies have been conducted to address the dust charging in subsonic flows [20, 23, 35, 36]. In recent studies the role of drag force in the dust alignment in subsonic flows has been addressed [37, 38]. However, there are still many open questions regarding the subsonic regime. For example, in supersonic flows, the decharging of the downstream grain in the wakefield is important for the system dynamics and stability and it has been shown that this effect is nearly linear with respect to the flow speed and with respect to the intergrain distance [27]. If this linear behaviour can be applied to the subsonic regime, it would also facilitate the modelling of dust dynamics in subsonic regimes [36]. Finally, in subsonic flows, the plasma particle trajectories may be non-trivial due to strong electric fields in the vicinity of grains. Thus, they may affect the dust charging in various multi-grain systems.

The modelling of dust grains in subsonic plasma flows poses some challenges: with an analytical approach one should account for nonlinear phenomena and self-consistent charging of many dust grains, while numerical simulations with methods that include a finite spatial grid can be difficult due to the stability of a simulated system. Systems with subsonic flows can become unstable due to physical instabilities, such as Pierce instability [39, 40], as well as numerical instabilities due to finite grid and particle weighting, such as the ringing instability for subsonic flows [41]. This could explain why so few numerical studies of dust charging in subsonic flows have been conducted in the past.

In this paper we push the limits of our numerical code DiP3D to study the charging of dust grains and wake effects in the range of accessible, numerically stable subsonic flow velocities. We consider a single grain, a pair of aligned grains, as well as multi-grain systems.

2. Numerical simulation

To study the charging of dust in subsonic plasma flows we use DiP3D, a 3D Particle-In-Cell (PIC) numerical code. The DiP3D code has been designed for studies of object-plasma interactions in various environments [22]. The details of the DiP3D code are available in previous works [27, 31] and here we provide only its main features in its basic version.

DiP3D is an electrostatic code that operates in a 3D Cartesian coordinate system. It simulates dynamics of electrons and ions in self-consistent force fields and can also account for plasma flows. The boundaries of the simulated system are open for plasma particles. Thus the particles can leave the simulation box, while new particles are introduced through the boundaries into the box according to the pre-computed flux. We use the Dirichlet boundary conditions at the edges of the simulation box for solving the Poisson equation. We find these boundary conditions to be applicable for the present study, provided that the simulation domain is large in terms of the Debye length and that the dust grains are far from the boundaries, i.e. when the plasma at the boundaries is affected very little by the charged dust.

Dust grains of spherical shape are introduced into the system, far away from the boundaries. The grains are charged self-consistently by plasma currents throughout the simulation. Since forces acting on plasma particles are smoothed due to the spatial grid, close to the grain surface we correct them by carrying out the direct force calculation with the P^{3}M-technique [42, 43]. This approach allows us to simulate dust grains with shapes that are independent of the grid structure, calculate proper dynamics of the plasma particles close to the dust surface and avoid self-forces due to the grid. We assume the dust grains to be rigid and immobile.

In the present study we simulate electrons and singly charged positive ions, with a mass ratio of numerical particles $m_i/m_e = 120$. Using reduced mass ratios is common in numerical plasma simulations as it allows speeding up the evolution of the system. We find that mass ratios $m_i/m_e > 100$ give credible results that are comparable in normalized units to the results with real mass ratios [44]. At the start of the simulation and at the boundaries of the simulation box, the velocities of plasma particles are assigned according to shifted Maxwellian velocity distributions. We use plasma density of $n = 10^{13}$ m^{-3}, electron temperature of $T_e = 3$ eV and electron to ion temperature ratio $T_e/T_i = 100$. The electron Debye length is $\lambda_{\mathrm{De}} = 4.03 \cdot 10^{-3}$ m.

We follow the dynamics of approximately 10^7 particles of each species with time resolution of $\Delta t < 0.01\omega_{\mathrm{pe}}^{-1}$, where ω_{pe} is the electron plasma frequency and run the code up to ten ion plasma periods τ_i. This is much longer than the time needed to reach stationary conditions for the charge on the dust (for supersonic flows this time is typically four τ_i). The simulated box is 5×10^{-2}m in each direction, with the grid spacing of $0.097\lambda_{\mathrm{De}}$. The radius of dust grains is $r \approx 0.1\lambda_{\mathrm{De}}$. Thus, we are in the same parameter regime that was used in our previous numerical experiment that considered supersonic flows [27].

The size of the grain is comparable to the grid spacing, but since we use the P^{3}M-technique, we can well resolve its shape and plasma dynamics in its vicinity. The size of the grain is large as compared to those in real experiments, which is a compromise between accuracy and computational effort. For smaller grains we find that the numerical noise in the charging characteristic of the grain becomes dominant. However, since the grain is still smaller than the Debye length, we see that the processes associated with the wake formation and the wake topology remain unchanged. For instance, the strength of the ion focus is determined by the plasma density and the charge of the dust grains, and we compensate higher dust charge by slightly lower plasma density. Note that experimental findings agree rather well with simulations of relatively large grains [34].

We concentrate on subsonic plasma flow velocities, where the speed of sound is defined as $C_s = \sqrt{kT_e / m_i}$. Subsonic flows are much slower than electron thermal velocity and they can also be considered in terms of flowing ions. For velocities $v_d \in [0.3, 0.5]C_s$, we find that the results for a single grain are not numerically stable, which we attribute to the ringing instability. Since we use the first order linear weighting on the grid, it seems consistent that the ringing instability sets in when $v_d \leqslant 0.5C_s$ [41]. Thus, the single grain results for $v_d \in [0.3, 0.5]C_s$ are not shown, as they are burden with large inaccuracy and possibly systematic errors. However for multigrain arrangements the simulations are stable for all flow velocities. For the completeness of discussion we also consider supersonic plasma flows, $v_d \leqslant 1.5C_s$.

3. Results

To study the effects of subsonic plasma flows on charging of multiple grain arrangements, we first consider a single grain and then continue with two grains aligned with the flow before addressing arrangements of 10 and 15 grains.

3.1. Single grain

In figure 1 we show the equilibrium charge q_s on a single grain from simulations with different flow velocities. The results are normalized to the absolute value of the charge on the grain in stationary plasma $q_0 = q(v_d{=}0)$ and the velocities to the sound speed C_s. The charge value on a grain gradually increases with the flow velocity within the considered velocity range. This charge increase is substantial already for subsonic flows, indicating that even a small break in the symmetry in the charging process can lead to a notable reduction of the ion collection current to the grain surface. This charge increase (i.e. the grain becomes more negatively charged) is due to reduction of the effective collecting area for ions. Note, that in agreement with standard theories [1, 26], the charge will reach a maximum at supersonic velocities and then decrease again, with the decrease at supersonic velocities that is due to increased ion flux to the grain surface at a fixed collection cross section [27]. In figure 1, the charge for subsonic velocities reaches up to double of the grain charge in stationary plasma. It does not change much with further increase in the velocity, indicating that the maximum charge is at $v_d > 1.5C_s$.

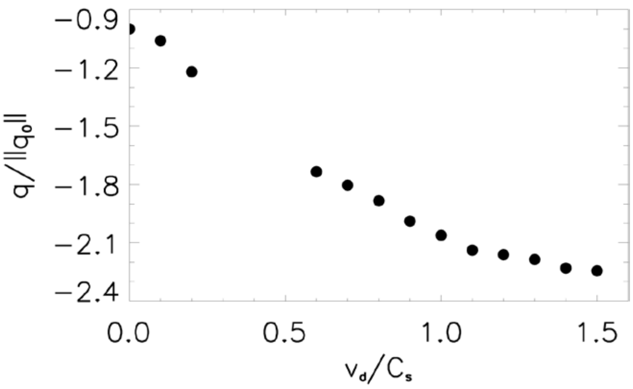

Figure 1. Charge q_s on a single grain, as a function of the flow velocity v_d. Results are for the data that is time averaged over three ion plasma periods for time-stationary conditions at the end of simulation. Charge q is normalized to the absolute value of the grain charge q_0 with vanishing flow velocity. Data points for $v_d \in [0.3, 0.5]C_s$ are omitted because they are affected by numerical instabilities.

3.2. Two grains

If the charge on a single grain depends that much on the flow velocity, one can expect, that the charge enhancement will have an effect on other grains, especially on downstream grains and their tendency to align in the direction of the flow. We have thus run a set of simulations with two grains aligned with the flow, where the flow velocity v_d and the distance $d \in (0.7, 1.3)\lambda_{\rm De}$ between the grains have been varied systematically.

When looking at the influence of a downstream grain on the charge on the upstream one, we see deviations from the charge on a single grain which are less than 3% in the supersonic regime and less than 5% in the subsonic regime. Thus for the considered intergrain distances d and plasma parameters, the influence of the downstream grain on the charging of upstream grain in the two-grain arrangement can be neglected in most of the studies.

However, the situation is completely different for the downstream grain. Already for supersonic flows the charge on the downstream grain was found to be reduced significantly [31]. For subsonic flow we observe the same trend. The results in figure 2(a) show the relative charge on the downstream grain q_2 with respect to the charge on the upstream grain q_1 as a function of relative distance d and flow velocity v_d. For a fixed v_d, the charge scales linearly with the intergrain distance, that is clearly seen in figure 2(b) where the relative charge is plotted as a function of d for selected v_d. Note that q_1 used for normalization changes with v_d. Thus each curve has been normalized to a different value of q_1. Note as well, that the previously shown linear scaling for supersonic flows [27], obviously holds even in the subsonic flow regime. Finally, figure 2 shows that the charge reduction increases with the flow velocity.

Thus, the charge on the downstream grain is clearly influenced by the wake effects. These wake effects are not only important for supersonic flows, but they are already significant for subsonic flows, where they cause notable charge reductions on the downstream grain only.

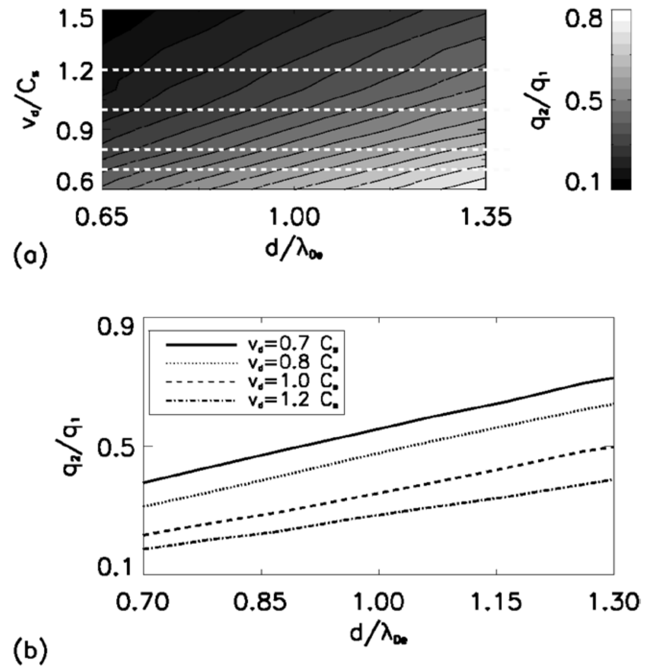

Figure 2. The charge q_2 on a downstream grain from the simulations of two grains aligned with the flow for different intergrain distances d and flow velocities v_d, normalized to the the charge on the upstream grain $q_1(a)$. In (b) the charge q_2 on the downstream grain is shown as a function of d for selected flow velocities v_d. The velocities are normalized to the speed of sound C_s and intergrain distances d to the electron Debye length λ_{De}. For completeness, results for supersonic flow velocities are also shown.

Modification of the charge on the downstream grain will have implications on the equilibrium distance between two dust grains aligned with the flow. The two charged grains will interact with each other and with the surrounding plasma. The downstream grain will in particular experience electrostatic force from the upstream grain and from the net positive charge due to the ion focus in the wake. Eventually, the grains will find the equilibrium position d_{eq}, at which the forces will balance each other. To find the equilibrium distance between the grains, we employ the model for finding the force f_2 acting on the downstream grain [27]:

$$f_2 = \frac{q_2}{4\pi\epsilon_0}\left(\frac{q_1\vec{r}_{1,2}}{r_{1,2}^3} + \int_0^d \int_A \frac{\rho\left(\vec{r}\right)\vec{r}_{\rho,2}}{r_{\rho,2}^3}\mathrm{d}\vec{r}\right). \qquad (1)$$

In this model, we account for the electrostatic force contribution from the charge q_1 on the upstream grain, as well as from the net positive charge, which is volume integrated in the wake region between the two grains. This model does not account for some other forces that can be present in the experiments, such as the gravity, ion drag, or forces due to confining potential. Nevertheless our force calculation is a reasonable approximation as gravity and confinement forces basically cancel, drag forces will only shift the grains further downstream, while the difference between the drag on different grains will increase the equilibrium distance. Thus, this simplified model provides a first estimate for the typical intergrain distance for grains aligned with the flow.

Table 1. Equilibrium distance d_{eq} between two grains aligned with the flow for different flow velocities v_d.

$v_d(C_s)$	0.6	0.7	0.8	0.9	1.0	1.1	1.2	1.3
d_{eq} (λ_{De})	0.78	0.78	0.87	0.97	0.97	1.0	1.07	1.07

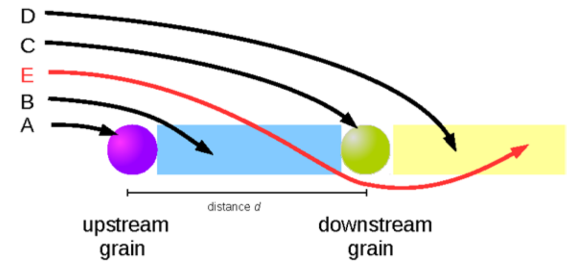

Figure 3. Schematic drawing of particle arrangement and different types of ion trajectories. Trajectories of type A and C end either on the upstream or on the downstream grain. Trajectories of type B only pass the wake region of the upstream grain (blue box). Trajectories of type D are those passing only the wake of the downstream grain (yellow box). Type E trajectories are special as they pass both wake regions.

The results are summarized in table 1. While for supersonic flows, d_{eq} is larger than the electron Debye length, for subsonic flows, the equilibrium distance is reduced to less than λ_{De}. The equilibrium distances all lie well in the simulated parameter regime (see figure 2).

To understand the charging process it is instructive to study the ion trajectories in the wake. For this purpose we distinguish five types of ion trajectories (see figure 3). Trajectories of type A and C are those which are responsible for the grain charging as they end either on the upstream or on the downstream grain. Trajectories of type B and D are those which only cross one of the wake regions. They contribute to the ion focus observed behind each grain. The fifth trajectory type (E) is special as it crosses both wake regions. We will refer to these types of trajectories and their color-coding in the following figures.

In figure 4 we show trajectories of sample cold ions for subsonic $v_d = 0.7C_s$ (a) and supersonic $v_d = 1.2C_s$ (b) flows. The results are for time-stationary conditions at the end of simulations and they are overplotted on the corresponding charge density plot in the x-y plane crossing the center of the grain. Only a small, central part of the simulation domain is shown, so that the wake is clearly demonstrated. The charge density is characterized by a strong maximum in the wake. This net positive charge density reflects the ion focusing by the grain, which is due to electrostatic lensing. The wake regions of the upstream (light blue box) and downstream (yellow box) are marked according to the color-code introduced in figure 3.

First, it is seen that the focus region in the wake of the upstream grain is due to ions deflected in the vicinity of that grain for both flow regimes. However, for the subsonic flow the ions passing the focus region are so strongly deflected that they can even travel against the flow after leaving the focus region. Second, figures 4(a)–(b) demonstrate that the focus region is less pronounced and less elongated for the subsonic case. In both cases the focus region behind the downstream grain

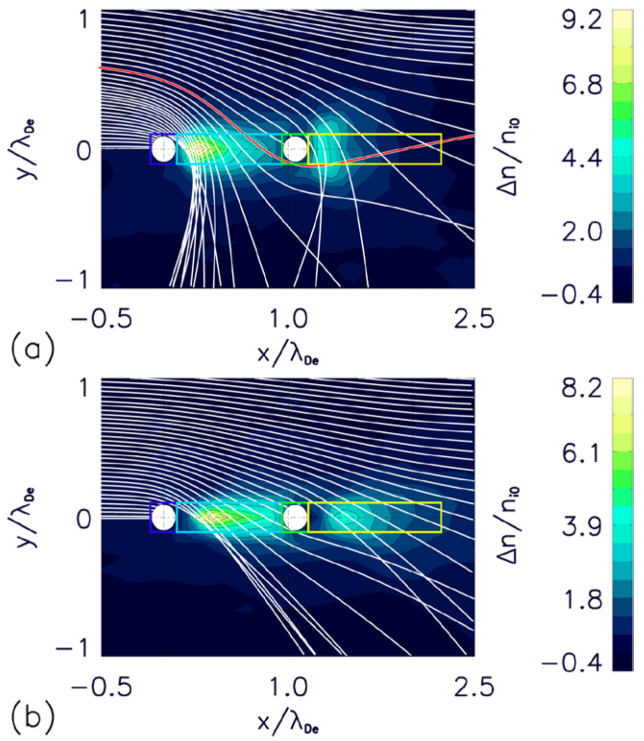

Figure 4. Charge density in the *x*-*y* plane through the centre of dust grains for two aligned grains with $d = 1.1\lambda_{De}$ with overplotted trajectories of sample cold ions for $v_d = 0.7C_s$ (*a*) and $v_d = 1.2C_s$ (*b*). Different regions of the wake are marked by rectangles, see text for details. Only a small, central part of the simulation domain is shown. The flow is in the positive *x*-direction.

is weaker and more diffuse. Finally, for both flow regimes, ions from the focus region of the upstream grain do not contribute much to the charging of the downstream grain. The main charging is due to ions being electrostatically lensed by the upstream grain directly to the downstream one and having a significant velocity component perpendicular to the average flow direction, see figure 4. While in the supersonic regime (figure 4(*b*)) only trajectories of types A–D are observed, we find type E trajectories for the subsonic case as well. The red trajectory in figure 4(*a*) proves that some of the ions entering the ions focus region of the upstream grain are passing the wake region behind the the downstream grain. Although, this *slalom* trajectory is not of importance for the charging, it is important for the momentum transfer to the grains and thus for the stability of the chain as discussed in [37].

Figure 5 visualizes the mapping of ions to the different regions in more detail. Here, the injection plane (*y*-*z*) for flowing cold ions is plotted. The colors indicate the region and thus the type of trajectory (see figure 3) where the particle injected at this *y*-*z*-position is mapped to. From these plots, we see that the respective regions upstream from the grains are well separated (their boundaries will slightly overlap for finite ion temperature). The exception is for subsonic flows, where the a thin red ring corresponds to ions that contribute to both ion density enhancements. In addition, the effective collection area for the ions decreases with increasing flow velocity, which will have effect on the grain charge (the grain charge becoming more negative, see figure 1). Further, note that for

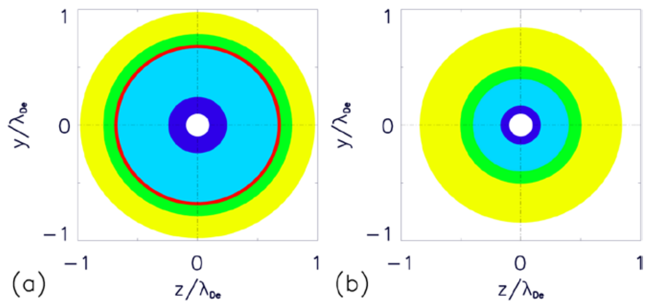

Figure 5. Regions in plasma in the *y*-*z* plane far upstream from the grains that correspond to the cold, flowing ions, whose trajectories would enter the regions marked in the charge density plot for $v_d = 0.7C_s$ (*a*) and $v_d = 1.2C_s$ (*b*). The particles in a yellow ring would enter a yellow box, etc. White circle in the center denotes the size of the grain. The red circle in (*a*) corresponds to ions that in the wake have *slalom* trajectories.

subsonic flows the light blue region, i.e. those ions are mapped to the focus region of the upstream grain, ends at about $0.7\lambda_{De}$. This is considerably larger than for supersonic flows (see figure 5(*b*)) and has implications for multi-grain systems.

3.3. Multi-grain systems

For the two grain-system we observe significant electrostatic lensing at both flow regimes, but in addition for subsonic flows we see that a significant fraction of ions is subject to large angle scattering giving rise to an upstream ion flow. Thus, subsonic flows should have important implications on the charging of grains in larger dust clusters. In this section we focus on the systems of 9 grains arranged in the layer, with one grain downstream in the wake and a system of 5 rods, each made of three grains.

Figure 6(*a*) shows the grain arrangement for the 9 + 1-system. The charge on the individual grains in this arrangement as a function of ion flow velocity is plotted in figure 6(*b*). The intergrain distance is set to $b = \lambda_{De}$. Thus, the Debye-spheres of individual particles overlap and the screening parameter $\kappa = b/\lambda_{De} = 1$ is typical for dust clouds. As a consequence the charges are not identical at $v_d = 0$. The charge is slightly more negative for particles with many nearest neighbors. Therefore, the charge of grain 1 is used as reference and all charges are normalized to $q_{1,0}$, i.e. its charge at $v_d = 0$.

Figure 6(*b*) clearly shows that the charge reduction of the downstream grain (grain 2) increases with v_d. At the same time the charge on all upstream grains increases. For supersonic flows all grains in the layer nearly have a similar charge, but as soon as we are in the subsonic regime, the charge on the grains differs. While the charges on grain 5 and 6 increase first, the same is observed later for grain 3 and 4 and last for the central grain (grain 1). Obviously, the number of nearest neighbors is of importance. Recalling figure 5, it is clear that for all flow conditions the collection radius is smaller than $0.5\lambda_{De}$. Thus, the collection areas (dark blue area) do not overlap and all grains could collect the same ion current. However, each grain will give rise to back-scattered ions at substantially low velocities (see figure 4(*a*)). These provide an additional ion current

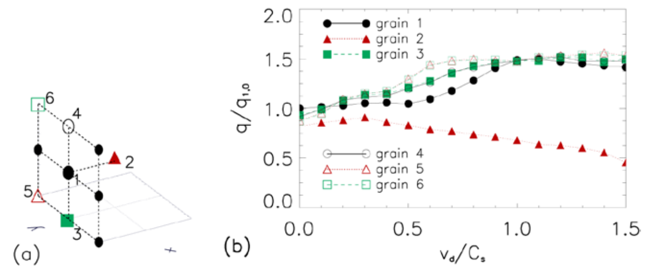

Figure 6. (*a*) Schematics of grain arrangements in the layer of nine grains and one downstream grain. (*b*) Charge on particular grains as a function of the flow velocity. The charge is normalized to the charge of grain 1 at conditions without the flow.

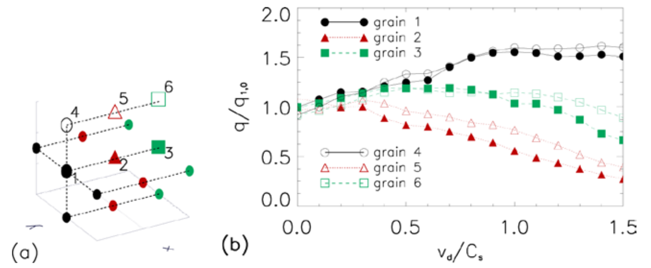

Figure 7. (*a*) Schematics of 15 grain arranged in five chains. (*b*) Charge on particular grains as a function of flow velocity, normalized to the charge on grain 4 at time-stationary conditions with no flow.

which will scale with the number of nearest neighbors. Note, that for $v_d = 0.7C_s$ the large angle scattered ions are mapped to the nearest neighbor position at $y = \lambda_{\mathrm{De}}$. Thus, in flowing plasma the central grain should have the lowest charge and the grains 5 and 6 at the corners the highest charge. However, the charging of grain 1 is typical for a grain in an infinite layer. Interestingly, its charge is constant for $v_d < 0.5C_s$ and $v_d > C_s$. Only in the regime $0.5C_s < v_d < C_s$, the charge increases by about 50 percent.

If we now compare the charge of grain 1 (upstream grain) and grain 2 (downstream grain), we observe that the initial charge difference (at $v_d = 0$), which is caused by overlapping Debye-spheres, remains almost unchanged up to $v_d = 0.3C_s$. For $v_d > 0.4C_s$ first indications of wake effects and additional ion currents due to lensing towards the downstream grain are observed. Instead of a further increase of charge (see upstream grains), its charge starts to decrease till a significant charge reduction is observed at supersonic flow conditions. Although, it should be noted that the charge reduction differs with respect to two isolated grains. For significant subsonic ion flows we observe a weaker ion focusing in the wake of grain 1, because the collection radius (see figure 5(*a*), light blue area) of an isolated grain is larger than $0.7\lambda_{\mathrm{De}}$ and thus the nearest neighbors in the layer truncate this to less than approximately $0.5\lambda_{\mathrm{De}}$.

A very similar charging characteristics is observed for 15 grains arranged in chains (see figure 7). The charge of the grains in the upstream layer gradually increases with flow velocity until it saturates at sonic velocities. The second layer is highly decharged by the upstream layer, due to strong ion focusing. Focus effects are observed for $v_d > 0.4C_s$. This matches the results of the 9 + 1-particle system well. It is interesting, that the charge reduction of the third layer is less than on the second. Obviously the low charge on the grains of the second layer results in a weak ion focus behind grains of the second layer. This characteristics is significant for both supersonic and subsonic flows, down to $v_d \approx 0.4C_s$.

4. Discussion

The significant change in the charge on the grain for subsonic flows, which is due to reduced ion collection cross section, has implications on the charging of downstream grains in this regime. The electrostatic lensing associated with ion focusing gives rise to enhanced ion density region in the wake and results in the reduction of the charge on the downstream grain. As shown in figure 2, for the two grains aligned with the flow, this charge scales linearly with the distance between grains in subsonic flows, within the considered velocity regime. The linear dependence on the charge on the downstream grain on the intergrain distance has been earlier reported for supersonic flows [27] and the charge reduction has been confirmed in experiments [34]. The fact that decharging of the downstream grain follows the linear scaling with the distance also for subsonic flows regime can largely facilitate modeling of larger dusty plasma systems in subsonic flows [36]. The same approach and analysis can be therefore used in both flow regimes. Furthermore, this indicates that both the ion focusing and wake effects are already substantial for subsonic flows and there seem not to be a very clear boundary for the charging characteristics and mechanisms between the two flow regimes in collisionless plasmas. Note that with further decrease of the flow velocity, the relative charge on the grains goes towards unity for larger distances. This is to be expected, as in the limit of very slow velocities and large distances the grains should charge independently and acquire equal charge.

For both subsonic and supersonic flows, decharging of the downstream grains is primarily due to ions being electrostatically lensed by the upstream grain, as it is also indicated in figure 4. The ion focus region will have an effect on the equilibrium position of the downstream grain, but unless the intergrain distance is small enough, these ions will not contribute significantly to the charging of the downstream grain. The effective collection area for the downstream grain will change with the flow velocity (see again figure 5) and for subsonic flows its radius will be in general larger than $\lambda_{\mathrm{De}}/2$. Thus, in systems with extended dust layers perpendicular to the flow, it is expected that charging of the downstream grain can be significantly different for sub- and supersonic ion flows.

A significant feature of the self-consistent charging in subsonic flows is the presence of *slalom* trajectories. Some ions that enter the ion focus region of the upstream grain are electrostatically lensed into the focus region of the downstream grain, see again figure 4. These slalom trajectories of ions will contribute to the perpendicular drag force and will have implications on the stability and alignment of the system of two grains. This mechanism has also been recently discussed in [37] and the role of perpendicular component of the drag force has been addressed in PIC simulations [38], although the latter did not account for self-consistent charging of the dust grains. While for supersonic flows the momentum transfer from an ion to the downstream grain will be larger, for subsonic flows the larger collection will imply a significant net momentum transfer to the grain. Notably, in subsonic flows, the slalom trajectories will have an impact on the stability of the system.

The charging of a downstream grain (grain 2) in the system of 9 + 1 grains, can be considered as an example of the grain charging behind an extended layer of dust. In this case the collection cross section for that grain will be determined by a Wigner cell within the layer [1]. The geometric effect due to the presence of the neigbors is important, in particular in the subsonic flow regime. Here the effective collecting area that would otherwise be larger than λ_{De}, is limited to the interparticle distance in the layer. The charge on the grain remains approximately constant for the wide range of subsonic flow velocities and it starts to decrease for $v_d > 0.5C_s$. Thus, the geometric effect limiting the effective collection area influences the charge on the downstream grain.

On the other hand, the charge on grain 1 in the system of 9 + 1 is approximately constant for subsonic velocities $v_d \leqslant 0.5C_s$. This is attributed to a strong back-scattering of ions in that regime. The collective response of the cluster can be considered as a large charged object and it is characterized by a strong potential enhancement in the wake. Both the potential enhancement and the neighboring charged grains will contribute to the scattering of ions. In the subsonic flow regime there is a significant number of ions that compensate for the reduced collection cross section on grain 1, while the number of back-scattered ions is less for other grains, for which the charge value slowly increases. For $v_d > 0.5C_s$ the population of backscattered ions is gradually reduced and the charge on all the grains increases. The geometry of the cluster implies that the charge increase is fastest for grains with the least number of neighbors (i.e. grains 5 and 6) and slowest for grain 1. For supersonic flows the charge on all upstream grains is approximately the same and the charging characteristics flattens already at $v_d = 1C_s$. The flow regime of $v_d \in (0.5, 1.0)C_s$ is thus an interesting one, where the most inhomogeneities in the charge distribution can be expected.

The charging mechanisms for dust strings is different. Here, the fraction of back-scattered ions is reduced due to the extension of the dust cluster in the flow direction and the corresponding shift of the potential enhancement further downstream. Thus, already for subsonic flows the grains in the upstream layer (grain 1 and 4) follow a similar characteristic and the charge difference for $v_d \in (0.5, 1.0)C_s$ is significantly reduced, also due to the fact that the number of nearest neighbors is only four for grain 1 in this cluster. Consistent with the picture for two grain aligned with the flow, already for $v_d > 0.5C_s$ the charge on the middle layer is significantly lower than that on the upstream grain. However, an important effect is that the charge on the third layer is almost constant for the subsonic flows and remains significantly less decharged in the supersonic regime. Seemingly, in the subsonic regime, the two first layers significantly disturb the flow and the last layer is effectively charged in more homogeneous plasma conditions.

Thus, our simulations clearly show that the charging process of grains significantly depends on the grain arrangement. However, we would like to recall that our simulations are based on some simplifications. First, we studied flowing ions which is not the same as sheath conditions. Second, we focused on collisionless plasmas. Third, the grains are rather large and at fixed positions. Thus, our results are not directly applicable to experimental situation. However, the observed charging processes are expected to play a role for small grains. As a consequence future investigations should carefully check whether the frequently used one-component approach for dust clouds is really valid and whether OML-theory or other isotropic charging models yield resonable charge approximations.

5. Conclusions

To conclude, our simulations of several dust grains embedded in a collisionless plasma with fowing ions show that the grain charge depends significantly on the detailed grain arrangement. We find that the grain charge of downstream grains is altered by the wake effects for supersonic as well as for subsonic ion flows. For specific flow conditions at subsonic velocities we even find that the charge of neighboring grains in a layer is influenced by backscattered ions. Thus, our results show that an identical charge on all grains in many-grains arrangements should not be expected as soon as ion flows are present.

Acknowledgments

We gratefully acknowledge financial support by Deutsche Forschungsgemeinschaft: SFB-TR24 project A3b.

References

[1] Fortov V E, Ivlev A V, Khrapak S A, Khrapak A G and Morfill G E 2005 *Phys. Rep.* **421** 1
[2] Morfill G E and Ivlev A V 2009 *Rev. Mod. Phys.* **81** 1353
[3] Shukla P K and Eliasson B 2009 *Rev. Mod. Phys.* **81** 25
[4] Piel A and Melzer A 2002 *Plasma Phys. Control. Fusion* **44** R1
[5] Ishihara O 2007 *J. Phys. D: Appl. Phys.* **40** R121
[6] Shukla P K and Mamun A A 2002 *Introduction to Dusty Plasmas* (Bristol: Institute of Physics Publishing)
[7] Vladimirov S V, Ostrikov K and Samarian A A 2005 *Physics and Applications of Complex Plasmas* (London: Imperial College Press)
[8] Melzer A, Schweigert V A and Piel A 1999 *Phys. Rev. Lett.* **83** 3194
[9] Hebner G A and Riley M E 2004 *Phys. Rev.* E **69** 026405
[10] Samarian A A, Vladimirov S V and James B W 2005 *JETP Lett.* **82** 758
[11] Kroll M, Schablinski J, Block D and Piel A 2010 *Phys. Plasmas* **17** 013702
[12] Block D, Carstensen J, Ludwig P, Miloch W J, Greiner F, Piel A, Bonitz M and Melzer A 2012 *Contrib. Plasma Phys.* **52** 804
[13] Ivlev A V, Morfill G and Fortov V E 1999 *Phys. Plasmas* **6** 1415

[14] Khrapak S A, Ivlev A V, Zhdanov S K and Morfill G E 2005 *Phys. Plasmas* **12** 042308
[15] Lampe M, Joyce G, Ganguli G and Gavrishchaka V 2000 *Phys. Plasmas* **7** 3851
[16] Lampe M, Joyce G and Ganguli G 2005 *IEEE Trans. Plasma Sci.* **33** 57
[17] Ludwig P, Miloch W J, Kählert H and Bonitz M 2012 *New J. Phys.* **14** 053016
[18] Willis C T N, Coppins M, Bacharis M and Allen J E 2012 *Phys. Rev.* **83** 036403
[19] Lapenta G 1999 *Phys. Plasmas* **6** 1442
[20] Maiorov S A, Vladimirov S V and Cramer N F 2000 *Phys. Rev.* E **63** 017401
[21] Miloch W J, Vladimirov S V, Pécseli H L and Trulsen J 2008 *Phys. Rev.* E **78** 036411
[22] Miloch W J 2010 *Plasma Phys. Control. Fusion* **52** 124004
[23] Hutchinson I H 2005 *Plasma Phys. Control. Fusion* **47** 71
[24] Hutchinson I H 2011 *Phys. Plasmas* **18** 032111
[25] Allen J 1992 *Phys. Scr.* **45** 497
[26] Whipple E C 1981 *Rep. Prog. Phys.* **44** 1197
[27] Miloch W J and Block D 2012 *Phys. Plasmas* **44** 123703
[28] Vladimirov S V and Nambu M 1995 *Phys. Rev.* E **52** R2172
[29] Ishihara O and Vladimirov S V 1997 *Phys. Plasmas* **4** 69
[30] Miloch W J, Trulsen J and Pécseli H L 2008 *Phys. Rev.* E **77** 056408
[31] Miloch W J, Kroll M and Block D 2010 *Phys. Plasmas* **17** 103703
[32] Steinberg V, Sutterlin R, Ivlev A V and Morfill G 2001 *Phys. Rev. Lett.* **86** 4540
[33] Melzer A, Schweigert V A, Schweigert I V, Homann A, Peters S and Piel A 1996 *Phys. Rev.* E **54** R46
[34] Carstensen J, Greiner F, Block D, Schablinski J, Miloch W J and Piel A 2012 *Phys. Plasmas* **19** 033702
[35] Arp O, Goree J and Piel A 2012 *Phys. Rev.* E **85** 046409
[36] Patrick Ludwig H K and Bonitz M 2012 *Plasma Phys. Control. Fusion* **54** 045011
[37] Piel A 2011 *Phys. Plasmas* **18** 073704
[38] Hutchinson I H 2011 *Phys. Rev. Lett.* **107** 095001
[39] Iizuka S, Saeki K, Sato N and Hatta Y 1979 *Phys. Rev. Lett.* **43** 1404
[40] Hur M S, Lee H J and Lee J K 1999 *IEEE Trans. Plasma Sci.* **27** 1449
[41] Brackbill J U 1988 *J. Comput. Phys.* **75** 469
[42] Hockney R W and Eastwood J W 1988 *Computer Simulation Using Particles* (Bristol: IOP Publishing)
[43] Matyash K, Schneider R, Ikkurthi R, Lewerentz L and Melzer A 2010 *Plasma Phys. Control. Fusion* **52** 124016
[44] Miloch W J, Pécseli H L and Trulsen J 2007 *Nonlinear Process. Geophys.* **14** 575